Numerical study of the effect of the leading edge shape on cavitation around inducer blade sections

Olivier Coutier-Delghosa, Jean-Luc Reboud, Regiane . Fortes Patella

Numerical Study of the Effect of the Leading Edge Shape on Cavitation Around Inducer Blade Sections

Olivier COUTIER-DELGOSHA**, Jean-Luc REBOUD***
and Regiane FORTES-PATELLA****

A numerical study of the cavitation behaviour of two-dimensional hydrofoils simulating a section of an inducer blade is presented. Two leading edge shapes were chosen to approach rocket engine inducer designs. They were tested with respect to the development of sheet cavitation. The numerical model of cavitating flows is based on the 3D code FINE/TURBO™, developed by NUMECA International. The cavitation process is taken into account by using a single fluid model, which considers the liquid vapour mixture as a homogeneous fluid whose density varies with respect to the static pressure. Numerical results are compared with experimental ones, obtained in the CREMHyG large cavitation tunnel[1]. Pressure distributions along the foil suction side and the tunnel walls were measured for different cavity lengths. Total pressure measurements along the foil suction side allow characterizing the effects of cavitation on the liquid flow. Influence of the leading edge shape on the cavitation behaviour and comparison between experiments and numerical predictions are discussed.

Key Words: Numerical Simulations, Cavitation, Rocket Engine Turbo-Pumps, Inducers, Hydrofoils

1. Introduction

The prediction of the cavitation behaviour is of first importance for the design of rocket engine turbo-pumps. Indeed, this phenomenon results in strong unsteady forces acting on the pump components, and it may lead to substantial performance losses. The analysis of the vapour occurrence in the pump, as well as the study of the unsteady effects related to cavitation, could directly influence the pump inducer design.

Several studies based on multi-phase flow approaches were developed during the last 10 years[2],[3]. They lead now to the development of three-dimensional Navier-Stokes codes that take into account the cavitation process[4]-[7]. In this context, a numerical model, aiming to take into account the cavitation phenomenon in inducers geometry is developed in collaboration with SNECMA Moteurs and the French space agency CNES. The final objective is to provide assistance to the design and prevision of operating range of rocket engine turbo-pumps, taking into account the steady state and unsteady effects of cavitation. The model is based on the commercial code FINE/TURBO™, developed by NUMECA International[8]. To simulate the cavitation process, a single-phase flow model is implemented[9] based on previous studies in 2D[2],[10],[11].

The aim of the present paper is to evaluate the ability of the numerical model to take into account the influence of the leading edge shape on cavitation behaviour in inducer geometries. The study concerns two hydrofoils simulating a section of an inducer blade, held in a cavitation tunnel with two different angles of attack. They are characterised by two different leading edge geometries, chosen to approach rocket engine inducer design[1]. Experimental results are compared with 2D computations in the different cases. A three-dimensional simulation of the complete hydrofoil geometry is also performed in one case, to illustrate the 3D effects on the cavitation sheet.

** LEGI/INPG, BP 53, 38041 Grenoble cedex 9, France. E-mail : coutier@hmg.inpg.fr
*** LTDS/ENISE, 58 rue J. Parot-42023 St Etienne cedex 2, France. E-mail : reboud@enise.fr
**** LEGI/INPG, BP 53-38041 Grenoble cedex 9, France. E-mail : fortes@hmg.inpg.fr

Nomenclature

C_p : pressure coefficient ($=(P-P_{ref})/(1/2\rho V_{ref}^2)$)
L_{cav} : cavity length (m)
L_{ref} : reference length (=chord of the foil) (m)
V : velocity (m/s)
V_{ref} : reference velocity (=inlet flow velocity) (m/s)
P : static pressure (Pa)
P_{ref} : reference pressure (=inlet static pressure) (Pa)
P_v : vapour pressure (Pa)
σ : cavitation number ($=(P_{ref}-P_v)/(1/2\rho V_{ref}^2)$)
ρ : liquid density (kg/m^3)

2. Experiment

The experimental study of the cavitation behaviour of two-dimensional hydrofoils simulating a mid-span section of an inducer blade has been performed in the large cavitation tunnel of the CREMHyG laboratory (Fig. 1)[1].

The upper and lower walls of the cavitation tunnel have been designed to generate along the suction side of the foil a pressure distribution as close as possible to the one existing along the inducer blade in non-cavitating condition. The hydrofoil chords are 0.9 meter long and their maximum thickness is about 14 mm. A 5 mm thin streamlined leg, through which pressure taps have been drilled, holds the foils. The reference flow velocity V_{ref} and static pressure P_{ref} are measured in the upstream rectangular section S_{ref} (137×120 mm^2), located at 200 mm upstream the foil leading edge. Those reference values are used to define the cavitation number σ. The maximum inlet flow velocity V_{ref} may be larger than 30 m/s. No marked effect of the amount of air dissolved in water has been observed on developed cavitation. During the present experiments, the air content of the water has been kept near saturation.

The behaviours of two different leading edges have been compared with respect to the development of sheet cavitation. Their shapes are reported on Fig. 2. The first leading edge presents a parabolic shape, about 3 mm long, creating with the suction side a sharp ridge. It simulates a blade whose upstream end has been bevelled. The second one is sharper and its rounded upstream end, where the cavity detachment occurs, presents a small curvature radius close to 0.2 mm. The two profiles will respectively be named hereafter "bevelled leading edge" (BLE) foil and "sharp leading edge" (SLE) foil. The second hydrofoil is 3 mm shorter than the first one and its relative thickness is a little smaller, but their two suction sides are identical.

Two different angles of attack have been tested: 4.1 and 4.5 degrees. They have been chosen to provide flow conditions close to those predicted in a blade-to-blade channel of the inducer at its nominal operating point. Because of the small ratio between the tunnel height and the chord length, the 0.4 degrees difference has a great influence on the cavitation behaviour.

Pressure measurements have been performed along the foils suction side (10 taps) and the tunnel walls (3 taps in the reference section, 7 along the lateral and lower walls and 4 along the upper wall). Pressure taps are connected with 1 mm diameter Polyamide pipes to piezo-resistive transducers with accuracy better than +/−0.1% of the 5 bar range.

The flow rate is measured by an electromagnetic flow meter, with a relative accuracy of 0.2%. The combination of inaccuracies on pressure and velocity measurements ensures on the pressure coefficient C_p and on the cavitation number σ a global uncertainty of +/−0.02 at $V_{ref}=10$ m/s.

Total pressure measurements have been performed using a 4 holes probe along 3 axes crossing the upper channel at 37%, 70% and 95% of the chord from the leading edge (Fig. 1). Velocities have been deduced from the total and static pressure measurements. Comparisons with LDA data acquired along the same axes were used to validate the method under non-cavitating and cavitating conditions.

3. Physical Model

Two-phase flow models are based on the assumption that the fluid is present in the computational

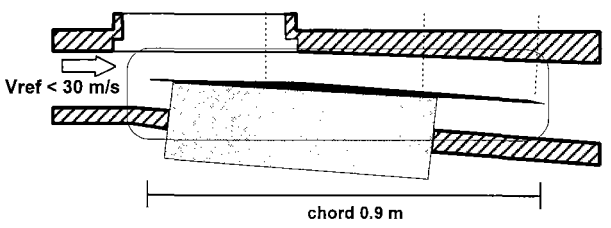

Fig. 1 Large cavitation tunnel (width=0.12 m) and inducer type blade section

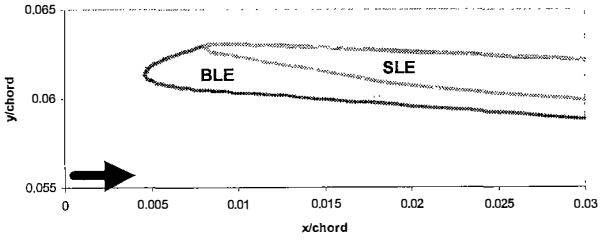

Fig. 2 Geometry of the bevelled leading edge (BLE) and the sharp leading edge (SLE). Angle of attack= 4.5 degrees

domain both as liquid and vapour. The vapour is characterized by the density ρ_v and the liquid by the density ρ_l. On each cell of the mesh, the unknowns are calculated for each phase, by averaging them on the volume occupied respectively by liquid and gas [for example: Ref.(12)].

In the present work, we apply a single fluid model based on previous numerical and physical work developed in LEGI[2),(11)]. It considers only one fluid, characterized by a density ρ that varies in the computational domain according to a state law. When the density in a cell equals the liquid one ρ_l, the whole cell is occupied by liquid, and if it equals the vapour one ρ_v, the cell is full of vapour. Between these two extreme values, the cell is occupied by a liquid/vapour mixture that we still consider as one homogeneous single fluid. The void fraction $\alpha = (\rho - \rho_l)/(\rho_v - \rho_l)$ corresponds to the local ratio of vapour contained in the mixture. In this simple model, the void ratio α is related to the state law, the fluxes between the phases are treated implicitly, and no supplementary assumptions are required.

Moreover, concerning the momentum fluxes, our model assumes that locally (in each cell), velocities are the same for liquid and for vapour: in the mixture regions gas structures are supposed to be perfectly carried along by the main flow. This hypothesis is often assessed for this problem of sheet-cavity flows, in which the interface is considered to be in dynamic equilibrium[6),(13),(14)]. The momentum transfer between the phases is thus strongly linked to the mass transfer.

In the present work the empirical barotropic law $\rho(P)$ used is presented in Fig. 3. When the pressure is respectively higher or lower than the vapour pressure, the fluid is supposed to be purely liquid or purely vapour, according respectively to the Tait equation and to the perfect gas law. The two fluid states are joined smoothly in the vapour-pressure neighbourhood. It results in the evolution law characterized mainly by its maximum slope $1/A_{min}^2$, where $A_{min}^2 = \partial P/\partial \rho$. A_{min} can thus be interpreted as the minimum speed of sound in the mixture.

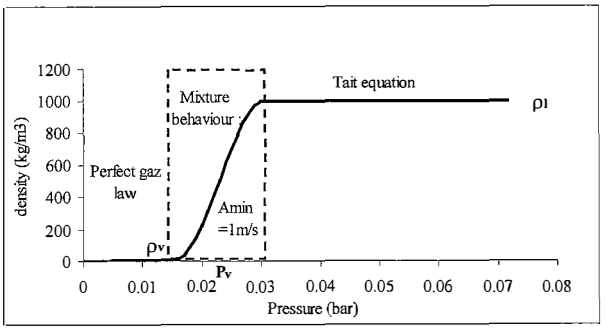

Fig. 3 The barotropic state law $\rho(P)$

4. Numerical Model

To calculate cavitating flows we apply the commercial code FINE/TURBO™ developed by NUMECA International. It is a three-dimensional structured mesh code that solves the time dependant Reynolds-averaged Navier-Stokes equations. A detailed description of the code is given in Ref.(8).

Unsteady calculations

Time accurate resolutions use the dual time stepping approach (see Ref.(15)). Pseudo-time derivative terms are added to the equations. They march the solution towards convergence at each physical time step. The code resorts to a multigrid strategy to accelerate the convergence, associated with a local time stepping and an implicit residual smoothing.

This kind of resolution is devoted to highly compressible flows. In the case of low-compressible or incompressible flows, its efficiency decreases dramatically. This well-known problem has been addressed by many authors and solved by introducing a preconditioner[8)]. This one is based on the studies of Refs. (16), (17). It consists in multiplying the pseudo-time derivatives by a preconditioning matrix Γ^{-1}. Such modifications have no influence on the converged result, since these terms are of no physical meaning, and converge to zero.

The discretization is based on a finite volume approach. We use a second order central scheme, which must be associated with two artificial dissipation terms, respectively of second and fourth order. The first one is activated in the strong pressure gradient areas, such as shocks. The other one is used in the whole domain, and it results in a second order space accuracy. The pseudo-time integration is made by a four-step Runge-Kutta procedure.

The physical time-derivative terms are discretized with a second order backward difference scheme that ensures a second order accuracy in time.

This numerical model was adapted to treat the cavitation process[9)]. The key point of this adaptation is the modification of the state law of the fluid. Our barotropic law implies the simultaneous treatment of two different cases: the fluid is highly compressible in the two-phase flow areas (the Mach number can be as high as 4 or 5) and it is almost incompressible in the pure vapour or pure liquid areas. So the main difficulty consisted in managing these two different states of the fluid, without creating any spurious discontinuity in the flow field. Besides, the cavitation consists in a very sharp and very rapid process. It means that the density time fluctuations and the density repartition must be smoothed, to avoid numerical instabilities. Thus, we use an under-relaxation of

the variations of the density to prevent too fast changing during one pseudo-time step. We also modified the switch between the two types of artificial dissipations. The second difference term is now also activated in the strong density gradient areas, such as cavitation sheet interface.

Turbulence model

We use for the calculations presented in this paper a classical Baldwin-Lomax turbulence model. Other calculations considering k-ε turbulence models are in progress to improve the physical analyses. A more detailed study of the influence of the turbulence model on unsteady cavitation simulation is proposed in Ref.(18). It shows a major effect of the compressibility effect modelling on the unsteady behaviour of cloud cavitation.

Boundary conditions

The boundary condition setting is based on a system of dummy cells. Classical incompressible types of boundary conditions are applied: imposed velocities at the inlet, and an imposed static pressure at the outlet. Numerical studies have been started in LEGI to improve these conditions, mainly by taking into account the test rig influence[19], but have not been applied in the cavitating case yet. Laws of the wall are applied along solid boundaries.

Initial transient treatment

First of all, a steady step is carried out, with a pseudo vapour pressure low enough to ensure no vapour presence in the whole computational domain. Then, this vapour pressure is increased progressively during the early time steps, until the required cavitation number σ is reached. Vapour appears progressively in the low static pressure regions during this transient. The cavitation number is then kept constant throughout the computation.

5. Two-dimensional Results

2D computations were performed on both geometries, for the two experimental angles of attack of 4.1 and 4.5 degrees. A 10 000 cells mesh was applied in the four cases (Fig. 4), and a large range of cavitation numbers was considered, according to the experimental results. In the case of the SLE foil at 4.5 degrees incidence, a second mesh has been tested, more refined near the leading edge.

In all computations a cavitation sheet appears on the suction side of the foil and completely stabilises as soon as the operating cavitation number is reached. Then, decreasing the cavitation number σ in successive steps allows drawing the relationship: cavitation number σ versus cavity length. Figures 5(a) and (b) present the results for the two angles of attack, respectively in the case of the BLE and SLE foils. Experimental results are also provided on these figures, to enhance comparison. We obtain a reliable agreement between numerical and experimental results, the case of the SLE foil at 4.5 degrees angle of attack needing nevertheless at particular treatment, as will be discussed hereafter.

4.1 degree angle of attack: experiments and computations confirm that the leading edge shape has

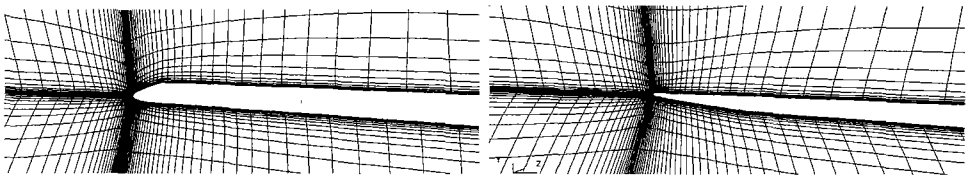

BLE SLE

Fig. 4 Detail of the mesh near the leading edges: BLE and SLE foil

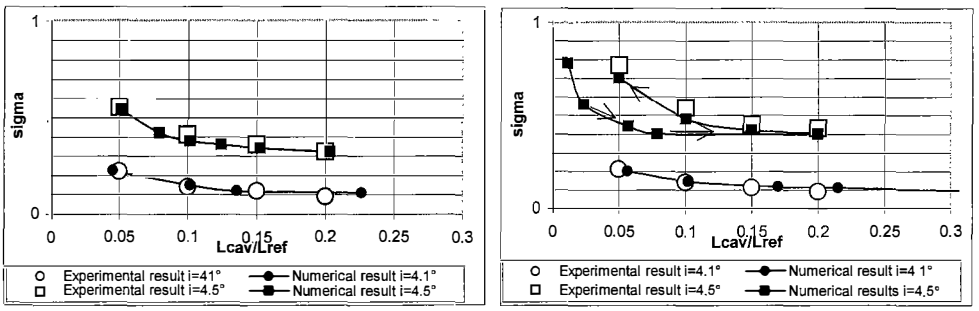

(a) (b)

Fig. 5 Cavitation number σ vs. (L_{cav}/L_{ref}) laws: (a) BLE foil; (b) SLE foil*
(* at 4.5 degrees, the arrow shows the succession of calculations)

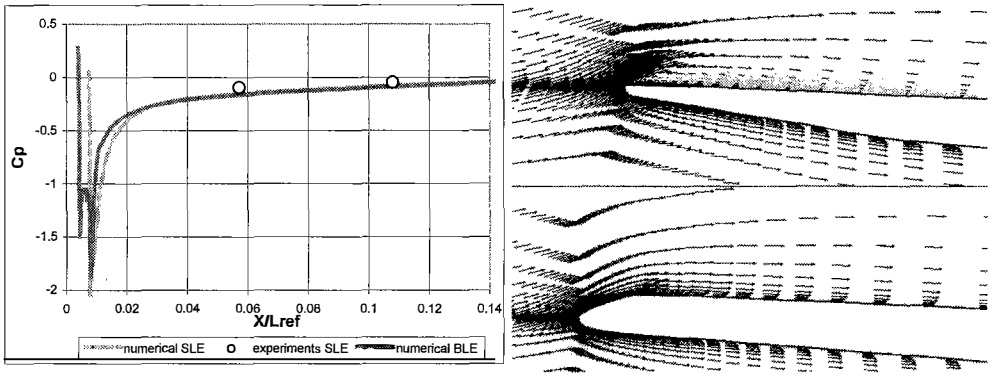

(a) (b)

Fig. 6 Comparison of numerical pressure distributions (a) and leading edge flow fields (b) for the two hydrofoils in non-cavitating conditions

almost no influence on the cavities length at low incidence. Visualisations with stroboscopic light show smooth and quasi-steady cavitation sheets at all the cavitation numbers tested. Only a short fluctuating wake downstream of the cavity is composed of small travelling vapour structures.

4.5 degree angle of attack : experimental observations report the unsteady behaviour of the cavities on the two foils, and a strong influence of the leading edge shape. At a given cavitation number σ, the mean cavity length is about two times larger on the SLE foil than on the BLE foil, and correspondingly for the same cavity length the cavitation number is about 25% higher. This effect was first not obtained in the numerical simulations with decreasing progressively the cavitation number : contrarily, it can be observed on Fig. 5(b) that very short cavities are predicted in the case of the SLE foil. That is why the computation was continued, re-increasing the cavitation number from the lowest value. A strong hysteresis phenomenon is then observed, the cavity remaining much larger during the re-increasing phase.

It can be seen on Fig. 6(a) that the pressure distribution obtained by the calculation along the suction side is the same on BLE and SLE foils, except for the 2% of the chord from the leading edge. The minimum pressure, which occurs very close to the leading edge, is a little lower on the SLE foil. The velocity fields calculated in non-cavitating condition are illustrated by Fig. 6(b). An area of separated flow can be seen in the case of the SLE foil. According to numerical simulations, the separated flow is progressively filled with vapour when the cavitation number is decreased. For low value of σ, the cavity length becomes much larger than the initial separated flow structure. While increasing again the cavitation number the cavity length remains larger than in the decreasing phase, and the agreement with experiment becomes much better.

In fact, the hysteresis phenomenon is not observed experimentally. The hysteresis predicted by the numerical calculations can be related to the physical and numerical models that do not well describe the shear effects of separated flows and do not capture the unsteadiness of the flow in cavitation region. Indeed, from the experimental point of view the cavities exhibit an unsteady behaviour associated with large vapour cloud shedding at 4.5 degree angle of attack for both hydrofoils. The numerical model fails to simulate this behaviour, and predicts a completely stable cavity. This current limitation of the model could be linked to the use of standard turbulence model[18]. Work is in progress to qualify various effects of the model used and of the numerical scheme, to improve the simulations of unsteady cloud cavitation behaviours.

Figure 7 shows the density of the fluid obtained for the four cases, for the cavitation number corresponding to a cavity length close to 15% of the chord. It can be noticed that the high angle of attack leads to a faster growing of the cavity thickness downstream of the detachment point, and to a larger void ratio along the foil surface.

Quantitative comparisons are investigated between experiments and the numerical results in the case of the bevelled leading edge at high angle of attack. The static pressure evolution along the profile is represented in Fig. 8 for a cavity length increasing from 5% of the chord to 20% of the chord.

We observe a general good agreement between the numerical results and the experimental data : the charts confirm that the cavity length is correctly predicted. The pressure downstream of the closure area is a little over-estimated by the calculation, which is mainly an effect of the 2D simulation that do not take into account the obstruction effects linked to

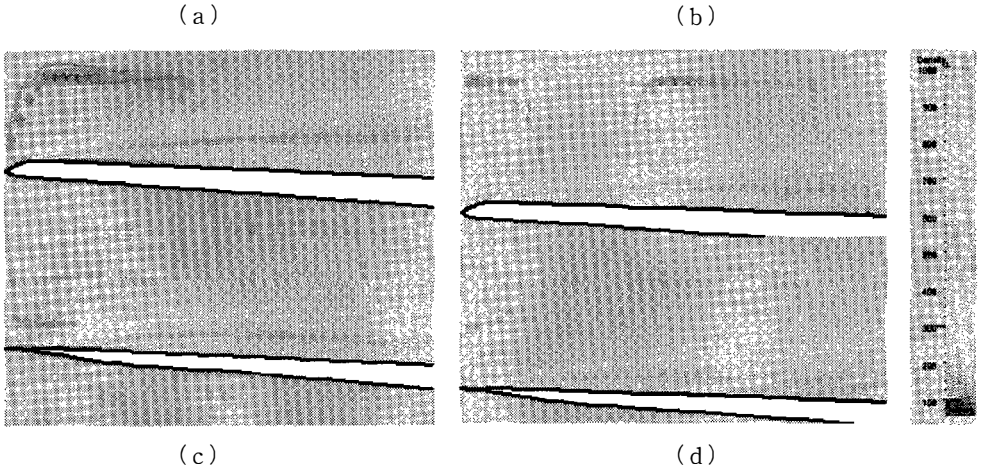

Fig. 7 Shape of the cavities with L_{cav}=15% L_{ref}, (a) Bevelled leading edge $-i$=4.5°, (b) Bevelled leading edge $-i$=4.1°, (c) Sharp leading edge $-i$=4.5°, (d) Sharp leading edge $-i$=4.1°

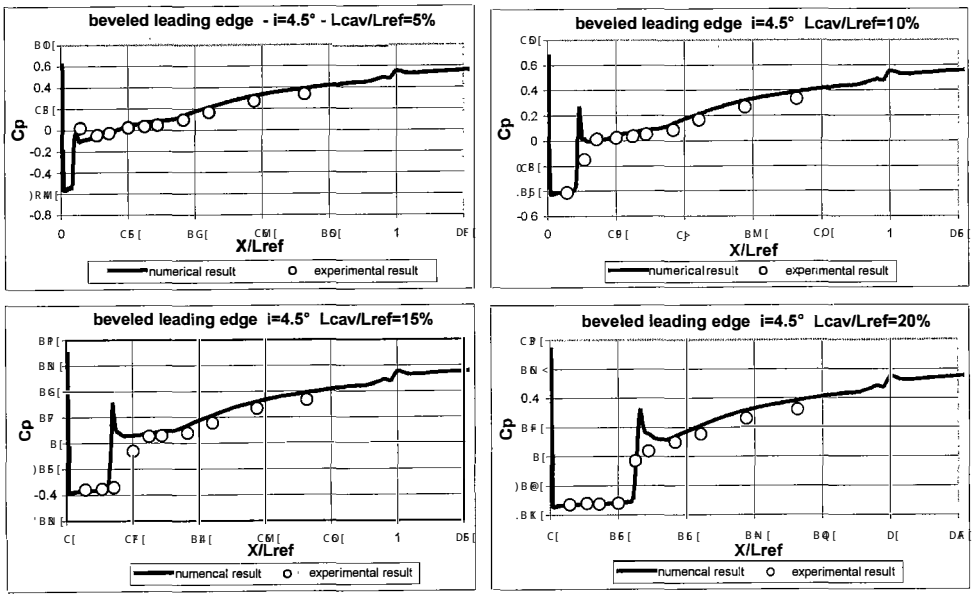

Fig. 8 Static pressure distribution on the profile : numerical and experimental results (BLE foil, V_{ref}=16 m/s)

the boundary layers developing along the sidewalls of the tunnel. Nevertheless, the most important discrepancy concerns the pressure increase in the cavity closure area, which appears more pronounced in the calculations than in the experiments. This sharp elevation predicted by the model in the cavity wake can be related to the complete stabilization of the cavitation sheet. The real behaviour involves self-oscillations of the cavitation sheet and the measured time-averaged pressure distributions downstream of the cavities appear smoothed.

Velocity profiles across the upper channel are more closely studied. The velocity distribution along three axes almost perpendicular to the foil suction side, respectively at 37%, 70%, and 95% of the chord length were investigated by means of a 4 holes probe. The component of the velocity vectors normal to these sections is represented in Fig. 9 in non-cavitating and cavitating conditions. The numerical results and the experimental data are compared. Because the obstruction effect due to the boundary layers along the sidewalls and along the leg holding the foil is not taken into account in the 2D simulation, the experimental mean velocity in the 3 sections are about 10% higher than the numerical ones. Then, in order to compare the profiles, all values have been divided by the mean velocity in non-cavitating condition.

In non-cavitating conditions, the boundary layer appears almost symmetric on both sides of the channel. In cavitating condition, the important increase of

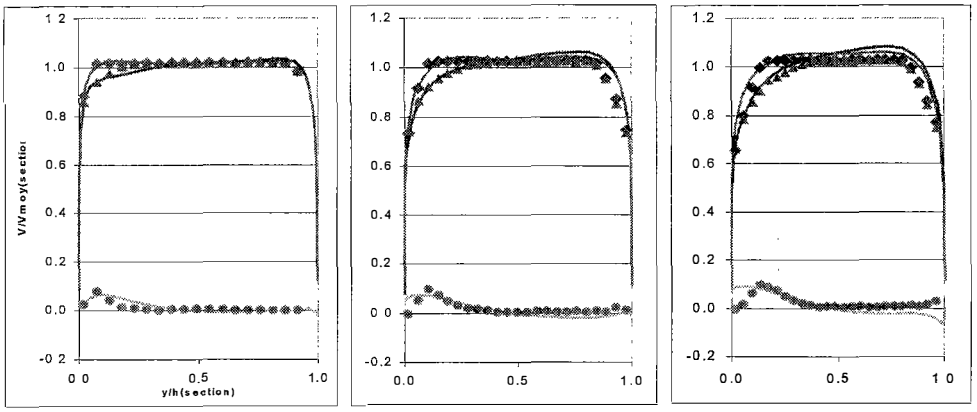

Fig. 9 Velocity profiles in three sections located respectively at 37%, 70%, and 95% of the chord. All values are divided by the mean velocity in the corresponding section in non cavitating condition. (BLE foil at 4.5 degree, V_{ref}=16 m/s). Non cavitating condition experimental points ◆; numerical result (full line); Cavitating condition (L_{cav}/L_{ref}=15%) experimental points ▲; numerical result (full line); Difference between non-cavitating and cavitating conditions experimental ●; numerical result (full line)

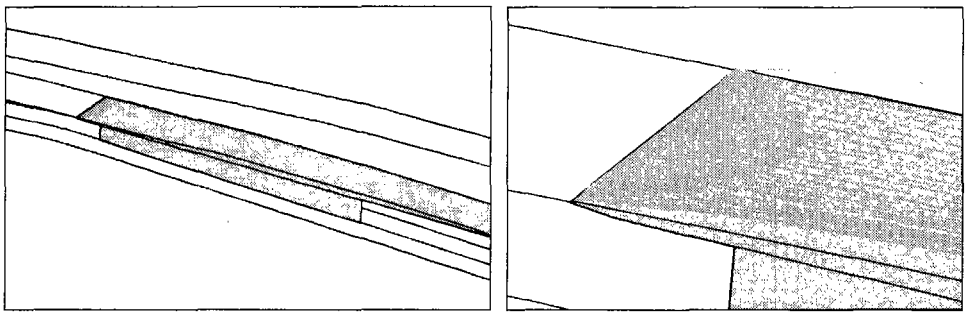

Fig. 10 Cavity shape: SLE foil, σ=0.02. Grey surface corresponds to a void ratio of 5%. Streamlines of the flow in the vicinity of the cavity surface are drawn in red

the displacement thickness due to the presence of the cavity wake is clearly visible all along the foil suction side (y/h=0). The interaction between the wake and the flow at the foil trailing edge leads to the slight decrease of the flow rate passing in the upper channel in cavitating conditions, which modifies a little the flow circulation around the foil and the resulting lift[1]. The agreement between measurement and simulation is satisfactory, in non cavitating and cavitating conditions. The quantitative influence of the cavitation sheet on the suction side boundary layer is notably well predicted.

6. Three-dimensional Computation

A three dimensional calculation taking into account the complete experimental geometry was performed, to illustrate the 3D ability of the numerical code and to estimate the effect of 2D simplifications applied in the previous cases. A 10^6 cells mesh of the SLE foil at 4.1 degrees angle of attack is used. The cavitation number is fixed to 0.2, which leads to a cavity length close to 5% of the chord. The cavity shape, shown in Fig. 10, is clearly three-dimensional, with an important influence of the sidewalls boundary layers, also visible on the streamlines drawn from the foil leading edge.

7. Conclusion

A numerical study of the cavitation behaviour of two-dimensional hydrofoils simulating a section of an inducer blade was presented. Two-dimensional computations were performed in different cases: two different foil leading edge shapes, two different angles of attack. A good agreement with experiments is generally obtained for the cavity length at different cavitation numbers. In one case, namely the sharp leading edge foil at the higher angle of attack, the presence of a separated flow near the sharp leading

edge, observed for non-cavitating conditions, creates the condition of a strong hysteresis phenomenon in the numerical result. Only the simulation performed by increasing the cavitation number from its minimum value provides a behaviour that conforms to experimental observations. With this angle of attack, the cavity is larger than with the bevelled leading edge foil, in both experiments and simulations. The self-oscillating behaviour of cavitation is not simulated at the present stage of the model. There is no effect of the leading edge shape at the lower angle of attack. Static pressure distributions along the foil suction side and velocity profiles in the cross sections of the foil suction side channel agree well with measurements. The presence of the cavitation sheet leads to the modification of the boundary layer all along the foil, with a probable effect on the trailing edge flow. A first 3D computation shows the influence of sidewall boundary layers on attached cavity.

Acknowledgements

This work is supported by a doctoral grant from the Education French Ministry MERT, SNECMA Moteurs (Rocket Engine Division), and by the French space agency CNES. The laboratory CREMHyG (Grenoble, France) provided experimental results.

References

(1) Reboud, J.L., Rebattet, C. and Morel, P., Effect of the Leading Edge Design on Sheet Cavitation around a Blade Section, Proc. of the 18th IAHR Symp. Hydraulic Machinery and Cavitation, Valencia, Spain, (1996).

(2) Delannoy, Y. and Kueny, J.L., Two Phase Flow Approach in Unsteady Cavitation Modelling, Proc. of Cavitation and Multiphase Flow Forum, ASME-FED, Vol. 98 (1990), pp. 153-158.

(3) Kubota, A., Kato, H. and Yamaguchi, H., A New Modelling of Cavitating Flows: A Numerical Study of Unsteady Cavitation on a Hydrofoil Section, J. Fluid Mech., Vol. 240 (1992), pp. 59-96.

(4) Takasugi, N., Kato, H. and Yamagushi, H., Study on Cavitating Flow around a Finite Span Hydrofoil, Proc. of Cavitation and Multiphase Flow Forum, ASME-FED Vol. 153 (1993), pp. 177-182.

(5) Alajbegovic, A., Grogger, H. and Philipp, H., Calculation of Transient Cavitation in Nozzle Using the Two-fluid Model, Proc. of the 12th Annual Conf. on Liquid Atomization and Spray Systems, Indianapolis, (1999).

(6) Kunz, R., Boger, D., Chyczewski, T., Stinebring, D. and Gibeling, H., Multi-phase CFD Analysis of Natural and Ventilated Cavitation about Submerged Bodies, Proc. of the 3rd ASME/JSME Joint Fluids Engineering Conference, San Francisco, (1999).

(7) Bunnell, R.A. and Heister, S.D., Three-dimensional Unsteady Simulation of Cavitating Flows in Injector Passages, J. Fluid Eng. Vol. 122 (2000), pp. 791-797.

(8) Hakimi, N., Preconditioning Methods for Time Dependent Navier-Stokes Equations, Ph.D. Thesis, Vrije Universiteit Brussels, Belgium, (1997).

(9) Coutier-Delgosha, O., Fortes-Patella, R., Reboud, J.L. and Hakimi, N., Numerical Simulation of Cavitating Flow in an Inducer Geometry, Proc. of the 4th European Conference on Turbomachinery, Firenze, Italy, (2001).

(10) Reboud, J.L. and Delannoy, Y., Two-phase Flow Modelling of Unsteady Cavitation, Proc. of the 2nd Int. Symp. on Cavitation, Tokyo, (1994).

(11) Reboud, J.L., Stutz, B. and Coutier, O., Two-phase Flow Structure of Cavitation: Experiment and Modelling of Unsteady Effects, Proc. of the 3rd Int. Symp. on Cavitation, Grenoble, France, (1998).

(12) Ishii, M., Thermo-fluid Dynamic Theory of Two-phase Flow, (1975), Eyrolles, Paris.

(13) Merkle, C.L., Feng, J. and Buelow, P.E.O., Computational Modelling of the Dynamics of Sheet Cavitation, Proc. of the 3rd Int. Symp. on Cavitation, Grenoble, France, (1998).

(14) Song, C.C.S. and He, J., Numerical Simulation of Cavitating Flows by Single-phase Flow Approach, 3rd Int. Symp. on Cavitation, Grenoble, France, (1998).

(15) Jameson, A., Time Dependant Calculations Using Multigrid, with Application to Unsteady Flows Past Airfoils and Wings, AIAA Paper 91-1596, (1991).

(16) Turkel, E., Preconditioning Methods for Solving the Incompressible and Low Speed Compressible Equations, Journal of Comp. Phys., Vol. 72 (1987), pp. 277-298.

(17) Choi, D. and Merkle, C.L., The Application of Preconditioning in Viscous Flows, Journal of Comp. Phys., Vol. 105 (1993), pp. 207-223.

(18) Coutier-Delgosha, O., Fortes-Patella, R. and Reboud, J.L., Evaluation of the Turbulence Model Influence on the Numerical Simulations of Unsteady Cavitation, Proc. of ASME FEDSM01, Cavitation and Multiphase Flow Forum, New Orleans, (2001).

(19) Longatte, F., Contribution à l'Analyse Phénoménologique des Ecoulements Instationnaires dans les Turbomachines: Etude du Couplage Pompe-Circuit et Rotor-Stator, Ph.D. Thesis, INPGrenoble, France, (1998).